

# Influence of Counterion Chemical Structure on Ionic Conductivity in Polymerized Ionic Liquids

Nathan Jude Rebello

## Abstract

Interest in a new class of electrolytes called polymerized ionic liquids has been growing in recent years, and the current goal in scientific literature is to explore mechanisms of ion motion and probe ways to increase the diffusivity and conductivity. In this work, molecular dynamic simulations were implemented in order to explore the effect of anion (or counterion) chemical structure on three important properties of ion mobility and ion transport: diffusivity (proportional to the conductivity), ion-association lifetime, and structural relaxation time. The eight counterions were bistrifluoromethylsulfonylimide (TFSI<sup>-</sup>), bispentafluoroethylsulfonylimide (PFSI<sup>-</sup>), tetrafluoroborate (BF<sub>4</sub><sup>-</sup>), tetrachloroaluminate (AlCl<sub>4</sub><sup>-</sup>), pentafluoroethylsulfate (PfO<sup>-</sup>), trifluoromethylsulfate (TfO<sup>-</sup>), and the chloride and bromide ions. The cation was poly(1-butyl-3-vinylimidazolium). Tetrachloroaluminate has the highest diffusivity and shortest structural relaxation time and ion-association lifetime. There is a negative correlation between structural relaxation time and diffusivity, and the physical meaning of the slope of this fit is explored.

## Acknowledgements

I would like to thank graduate student Jordan R. Keith (Department of Chemical Engineering) and supervisor Dr. Venkat Ganesan (Department of Chemical Engineering) for their support and guidance on this engineering honors thesis. Furthermore, I would like to thank Dr. Venkat Ganesan for his mentoring and support throughout my undergraduate career and Dr. Vaidyanathan Sethuraman, a former Ph.D. student in Chemical Engineering, for his guidance on past projects and for being a great teacher. I would like to acknowledge the Texas Advanced Computing Center (TACC) for providing the computing resources that have contributed to the results of this work.

# Dedications

I would like to dedicate this thesis to my parents for the support and encouragement they have given me, including in my research endeavors.

# 1 Introduction

Ionic liquids are salts that consist of cations or anions in liquid form. A cation is a molecule with a positive charge, and an anion is a molecule with a negative charge. Polymerized ionic liquids (polyILs) consist of cations or anions of traditional ionic liquids (ILs) in polymerized form. A schematic of a polyIL is displayed in Figure 1.[1] PolyILs have received great interest as a class of polymeric materials because they can combine favorable ionic transport features of ionic liquids with mechanical durability characteristic of solid polymerized electrolytes. In other words, polyILs have both strength and the ability to transport ions, and this is what gives rise to conductivity. The mechanical strength arises as polyILs consist of large polymerized molecules that are not able to move effectively, but they are surrounded by smaller counterions that are able to move rapidly and long distances in the system. Counterions, as defined in this work, are ions that diffuse rapidly and are not adhered to a polymer backbone. The unique chemical and mechanical properties of polyILs make them highly desirable for a diverse range of applications, including fuel cells, battery electrolytes, drug delivery, and electric double-layer capacitors.[2–7] Approaches to increase ionic conductivity without compromising mechanical strength are currently being undertaken for electrolytic applications.

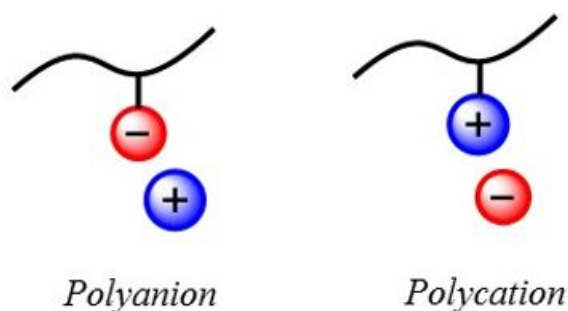


**Figure 1:** Schematic of a polymerized ionic liquid. Either the cation or the anion can be in polymerized form. The cation has a positive charge, and the anion has a negative charge.[1]

Over the years, there has been much literature on this subject regarding not only the proposed mechanisms of ion transport in polymerized ionic liquids but also how varying

different parameters can affect the diffusivity and conductivity. Mechanisms of ion transport need to be understood in order to develop highly conductive polyILs, and parameters including the length of the polymer backbone, the side chain linker length, the counterion and cation chemical structure, and the temperature and pressure can be varied. In literature, important design parameters in polyILs involve the chemical structure and composition of the anions and cations of traditional ionic liquids. Of the many cations studied, imidazolium was found to be one of the best for ionic conductivity.[7, 8] An imidazolium group is a five membered ring with two nitrogens and two double bonds, and a similar type cation is utilized in this work. Recent studies have probed the effect of alkyl side chain length and pendant linker length on conductivity, with longer alkyl side chains resulting in decreased conductivity and longer pendant linker lengths resulting in increased conductivity.[9–13] Furthermore, Choi [14] proposed a molecular volume effect on glass transition temperature, with smaller repeat unit molecular volume polyILs exhibiting higher glass transition temperatures. In a related study, Iacob [6] noted that interconnected polar domains, influenced by pendant lengths and counterion sizes, can be a key determinant in facilitating anion diffusion, with smaller counterion sizes and shorter alkyl side chain lengths preferred to achieving liquid electrolytes with higher conductivity. Lapan and Scheler [15] have shown ion-pair relaxation to play a key role in conductivity. These studies motivate the important question addressed in this work: How does the counterion chemical structure influence diffusivity and ion motion within the polyIL?

In this study, the cation is poly(1-butyl-3-vinylimidazolium). The counterions are divided into 4 groups based on chemical structure (Figure 2): tetrafluoroborate ( $\text{BF}_4^-$ ) and tetrachloroaluminate ( $\text{AlCl}_4^-$ ), chloride ( $\text{Cl}^-$ ) and bromide ( $\text{Br}^-$ ) ions, trifluoromethylsulfate ( $\text{TfO}^-$ ) and pentafluoroethylsulfate ( $\text{PfO}^-$ ), and bistrifluoromethylsulfonylimide ( $\text{TFSI}^-$ ) and bispentafluoroethylsulfonylimide ( $\text{PFSI}^-$ ). The abbreviated names of these chemicals are in parenthesis, and these specific molecules will be referred to by their abbreviated names. Perhaps as this project moves forward, more counterions can be selected with similar chemical structure. For instance, fluoride and iodide ions can be selected in addition to

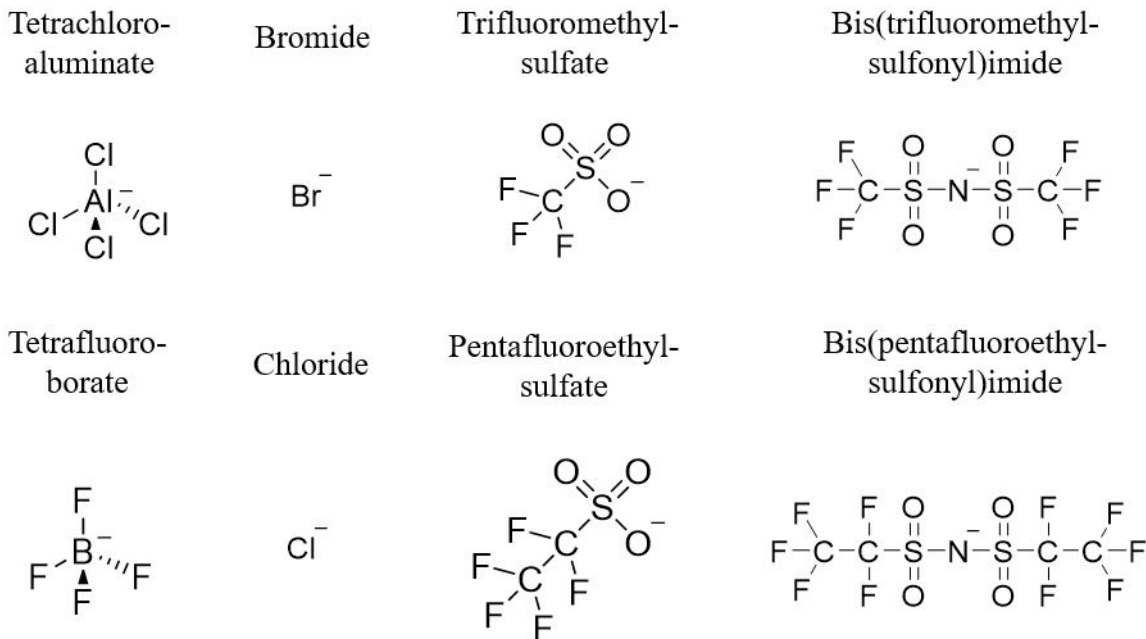


**Figure 2:** The counterions above were chosen for this work.

chloride and bromide ions. However, this work focuses specifically on these 8 counterions and important parameters related to ion mobility and ion transport are determined: diffusivity (proportional to the conductivity), structural relaxation time, and ion-association lifetime. These 8 counterions were chosen because inter- and intramolecular parameters are available or can be calculated for molecular dynamics simulations, and the meaning of the molecular parameters gathered from published data sets and the simulation methodology is explained in greater detail in Section 2. While diffusivity is an important parameter in ion mobility, the conductivity is more important to the design of materials; the Nernst-Einstein conductivity is proportional to the diffusivity of the counterions because the diffusivity of the polymerized cation is expected to be relatively small. Thus, the diffusivities reported in this work provide insight into the conductivity of these materials.

## 2 Methodology

Atomistic molecular dynamics (MD) simulations are employed to report the effects of counterion chemical structure at 3 different temperatures (500 K, 550 K, 600 K) on diffusivity, structural relaxation time, and ion-association lifetime in imidazolium based polyILs. This temperature range is a general temperature range for applications related to polymerized ionic liquids.[5, 6] Molecular dynamics simulations use the classical equations of motion to predict the location and movement of the counterions as they diffuse.[16] The equations that govern the motion of these counterions include Newton’s second law of motion (force equals mass times acceleration) and the relationship between force and potential energy (force equals the negative derivative of the energy with respect to position). Once the energy of the system is determined, then the forces acting on the molecules can be determined, and the positions of atoms at the next time step can be determined.

The following general interaction potentials were used in molecular dynamics simulations:[5]

$$U(r) = U^{bonded}(r) + U^{non-bonded}(r) \quad (1)$$

$$U^{non-bonded}(r) = 4\epsilon \left[ \left( \frac{\sigma}{r} \right)^{12} - \left( \frac{\sigma}{r} \right)^6 \right] + \frac{q_1 q_2}{r} \quad (2)$$

$$U^{bonded}(r) = k_r (r - r_0)^2 + k_\theta (\theta - \theta_0)^2 + \frac{1}{2} \sum_{n=1}^4 [K_n (1 + (-1)^{n+1} \cos(n\phi))] + K [1 - \cos(2\phi)] \quad (3)$$

In Equation 2, the first term describes the Lennard-Jones potential model. The Lennard-Jones potential has two main parameters: the depth of the curve ( $\epsilon$ ) that describes the strength of the interaction between the atoms and the distance ( $\sigma$ ) at which the potential is at 0. If the atoms are too close, the potential function becomes positive, and a force acts to separate the atoms. The second term in Equation 2 represents the Coulomb interaction

potentials in the system that are driven by charged particle (cation and anion) interactions. In Equation 3, the first term represents the energetic contributions to the system from bond stretching. Bonded energy interactions can be modeled as harmonic springs, and the energy interactions depend on a spring constant ( $k_r$ ) and the square of the difference of the distance of the atoms  $r$  from their equilibrium distance  $r_o$ . The farther the atoms are from their equilibrium distance, the more energy that exists, and a force will act to bring the atoms to their equilibrium distances. The second term represents the contribution from angle stretching and bending, which depends on constant  $k_\theta$  and the equilibrium angle  $\theta_0$ . The final two terms in Equation 3 represent the contributions from dihedrals and impropers.[5]

In this work, atomistic MD simulations were performed using LAMMPS molecular dynamics software package. In a given run at a specific temperature, the system will simulate the motion of counterions (anions) in the presence of polymerized cations. In order for the computer to predict the location and movement of the anions, the simulation requires an input file specifying the nature of the interactions in the system and a data file with constants quantifying the different energy interactions of the charged molecules (bonded coefficients, angular coefficients, dihedral coefficients etc.) and the starting position of the atoms. The input file specifies that the molecules are charged, the bonded and angular styles are harmonic, there exist periodic boundary conditions, and there are specific cutoff distances for Lennard-Jones interactions. In the data file, the total number of atoms is specified, as well as the number of different types of atoms and their respective masses (in this system nitrogen, carbon, hydrogen, etc.). Other parameters that are specified in the data file include the total number of bond types, angle types, and dihedrals, as well as specified constants for each. For example, in a simulation with PFSI<sup>-</sup> as the counterion, the data file specifies that there are 22,624 angles (75 different angle types) for 12,112 atoms. For each angle type, there are two parameters specified in Equation 3. In a simulation with TfO<sup>-</sup>, there are 8,768 bonds in the system and 43 bond types. For each bond type, there are two parameters in the harmonic spring equation in Equation 3. In summary, a comprehensive list of parameters is required, and these parameters can be gathered from the Optimized Potential for Liquid



Simulations data set (OPLS-AA) and other literature sources.[5, 17–23]

The diffusivity, structural relaxation time, and ion-association lifetime are computed in this work. The diffusivity is:

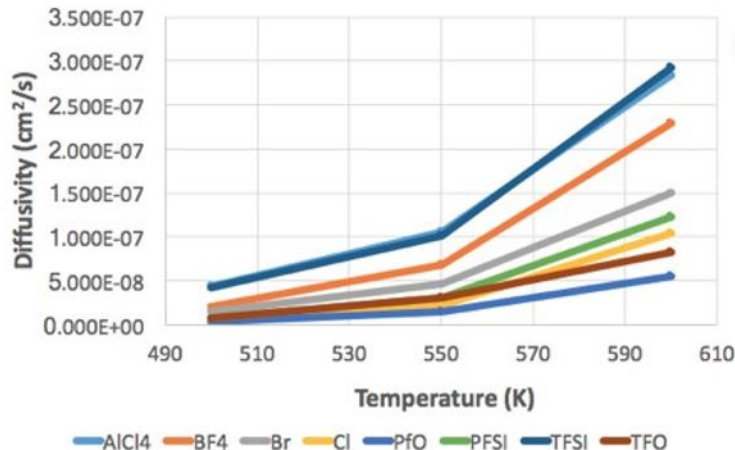
$$D = \lim_{t \rightarrow \infty} \frac{1}{6t} \langle (r(t) - r(0))^2 \rangle \quad (4)$$

where  $r(t)$  is the center of mass of the ion at a specific time. This limit can be estimated using the mean squared displacement versus time plot, and diffusivity can be computed for the linear portion of the plot. The structural relaxation time is a timescale associated with the intermittent time auto-correlation function. This involves determining if ion pairs are associated at the beginning and end of a time interval, but this does not consider ion pairs breaking apart and forming in the interval. The ion-association lifetime is associated with a continuous time auto-correlation function and involves computing how long ion pairs stay associated. These formulas can be found in literature.[4]

Section 3 shows the simulation results for the 8 counterions at 500 K, 550 K, and 600 K. For a counterion system at a specified temperature, there were 120 to 500 nanoseconds (ns) worth of simulated motion, and the amount of time for simulations depended on the linear fit of the mean squared displacement versus time plot. After the production runs were finished at 600 K, the system was cooled to 550 K for 40 ns and equilibrated for 10 ns before production runs at 550 K began. The system is isothermal and isobaric, and the number of atoms remain constant (NPT ensemble).

### 3 Results and Discussion

Figure 3 shows the diffusivity with respect to temperature for the 8 different counterions. On the  $y$  axis, the diffusivity is measured in  $\text{cm}^2/\text{s}$ , and on the  $x$  axis, the temperature is measured in Kelvin. Diffusivities are on the order of  $10^{-7}$ , which makes sense based on studies in literature.[5]



	500K	550K	600K
AlCl <sub>4</sub> <sup>-</sup>	1	1	2
BF <sub>4</sub> <sup>-</sup>	3	3	3
Br <sup>-</sup>	4	4	4
Cl <sup>-</sup>	7	7	6
PFO <sup>-</sup>	8	8	8
PFSI <sup>-</sup>	6	6	5
TFSI <sup>-</sup>	2	2	1
TFO <sup>-</sup>	5	5	7

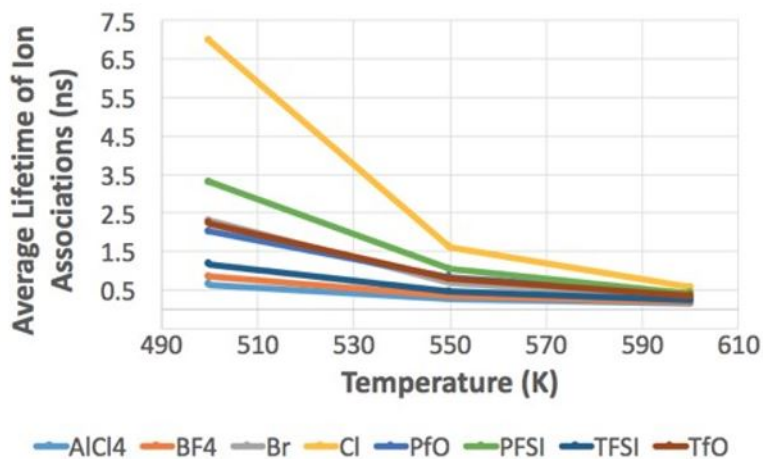
**Figure 3:** Diffusivity versus temperature for the eight counterions. The bottom table reveals the ranking of diffusivities from highest (1) to lowest (8) for each counterion at the 3 different temperatures. PFO<sup>-</sup> had the lowest diffusivity across all temperatures.

There are many interesting trends. As temperature increases, the diffusivity for all 8 counterions increases. This makes sense since at higher temperatures, molecules have more kinetic energy, and they are able to diffuse faster. The variance in diffusivities increases with temperature as well, indicating that temperature plays a critical role in driving counterion motion in some molecules more than others. Both the plot and the table in Figure 3 reveal that AlCl<sub>4</sub><sup>-</sup> and TFSI<sup>-</sup> have the highest diffusivities across all temperatures, while PFO<sup>-</sup> has the lowest diffusivity. For reference, at 500 K, AlCl<sub>4</sub><sup>-</sup> has a diffusivity of  $4.38 \times 10^{-8} \text{ cm}^2/\text{s}$ , while PFO<sup>-</sup> has a diffusivity of  $3.50 \times 10^{-9} \text{ cm}^2/\text{s}$ , nearly 13 times smaller. At 600 K, AlCl<sub>4</sub><sup>-</sup> has a diffusivity of  $2.84 \times 10^{-7} \text{ cm}^2/\text{s}$ , while PFO<sup>-</sup> has a diffusivity of  $5.52 \times 10^{-8} \text{ cm}^2/\text{s}$ ,

nearly 5 times smaller. There is some crossover in diffusivities as well. For example,  $\text{TfO}^-$  has a higher diffusivity than chlorine at 550 K, yet the opposite is true at 600 K. This is something worth exploring as we continue on this project. Perhaps at higher temperatures, chlorine and  $\text{PFSI}^-$  overtake  $\text{TfO}^-$  because temperature plays a greater role in the diffusivity for these counterions than it does for  $\text{TfO}^-$ .

Based on these results,  $\text{AlCl}_4^-$  has the highest or nearly highest diffusivity in all cases. It could be postulated that the tetrahedral geometry of the counterion enables it to pack more efficiently as it associates and interacts with the polycation, and this would allow the free counterions to have a less obstructed path as they diffuse. This hypothesis would explain the relatively high diffusivity for  $\text{BF}_4^-$ , which also has a tetrahedral geometry. However, this observation would not explain why  $\text{TFSI}^-$  has a relatively high diffusivity and  $\text{Br}^-$  and  $\text{Cl}^-$  have relatively low diffusivities, so perhaps there are other factors to consider. Coordination numbers for the different counterions will be computed; it is expected that  $\text{Br}^-$  and  $\text{Cl}^-$  have higher coordination numbers than  $\text{TFSI}^-$  and  $\text{PFSI}^-$ , and this future study will provide insight into the interactions between the counterion and cation. Moreover, it is expected that the association between the  $\text{AlCl}_4^-$  and the imidazolium group is relatively weak, allowing the  $\text{AlCl}_4^-$  to have a higher diffusivity. Motivated by this hypothesis, the association between ions is explored in Figures 4 and 5.

Figure 4 displays the ion-association lifetime, and Figure 5 reveals the structural relaxation time for the 8 counterions at the 3 different temperatures. In these plots, association time is measured in nanoseconds, and temperature is in Kelvin. As temperature increases, structural relaxation time and ion-association lifetime decrease. This makes physical sense; at higher temperatures, ions have more kinetic energy, and they remain associated for a shorter period of time. In Figure 4,  $\text{AlCl}_4^-$  has the shortest ion pair association at 600 K (0.15 ns), 550 K (0.25 ns), and 500 K (0.63 ns), and chlorine has the longest ion pair association at 600 K (0.57 ns), 550 K (1.61 ns), and 500 K (6.96 ns). In Figure 5,  $\text{AlCl}_4^-$  has the shortest structural relaxation time at 550 K (28.39 ns) and 600 K (8.65 ns) but not at

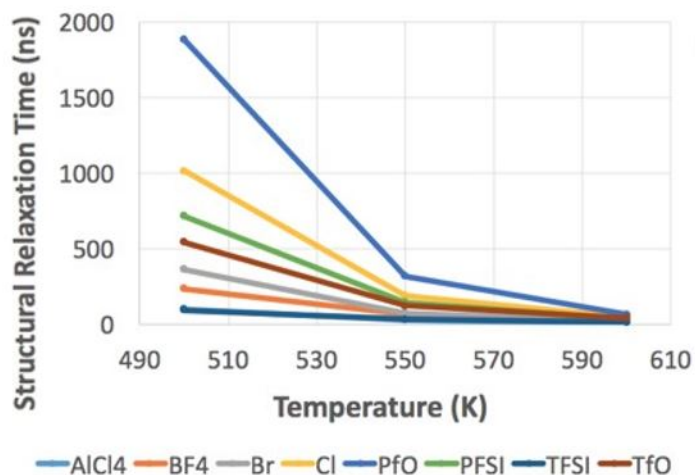


	500K	550K	600K
AlCl <sub>4</sub> <sup>-</sup>	8	8	8
BF <sub>4</sub> <sup>-</sup>	7	7	7
Br <sup>-</sup>	3	5	5
Cl <sup>-</sup>	1	1	1
PfO <sup>-</sup>	5	3	3
PFSI <sup>-</sup>	2	2	2
TFSI <sup>-</sup>	6	6	6
TfO <sup>-</sup>	4	4	4

**Figure 4:** Ion-association lifetime versus temperature for the 8 different counterions. The bottom table reveals the ranking at 3 different temperatures for each counterion from longest lifetime (1) to shortest (8).

500 K. At 500 K, TFSI<sup>-</sup> has the shortest structural relaxation time of approximately 93.80 ns while PfO<sup>-</sup> has the longest structural relaxation time at 600 K (62.43 ns), 550 K (315.31 ns), and 500 K (1879.29 ns).

There is an inverse correlation between structural relaxation time and diffusivity: PfO<sup>-</sup> has roughly a lower diffusivity and longer structural relaxation time; conversely, AlCl<sub>4</sub><sup>-</sup> has a higher diffusivity and a shorter structural relaxation time. Figure 6 shows a log-log plot. Indeed, there is a negative correlation between structural relaxation time and diffusivity, and the R<sup>2</sup> value is 0.99. The slope of the curve can provide insight into the physical



	500K	550K	600K
$\text{AlCl}_4^-$	7	8	8
$\text{BF}_4^-$	6	6	6
$\text{Br}^-$	5	5	5
$\text{Cl}^-$	2	2	2
$\text{PFO}^-$	1	1	1
$\text{PFSI}^-$	3	3	4
$\text{TFSI}^-$	8	7	7
$\text{TfO}^-$	4	4	3

**Figure 5:** Structural relaxation time versus temperature for the 8 different counterions. The bottom table reveals the ranking at 3 different temperatures from longest relaxation time (1) to shortest (8).

relationship between these variables. If the curve is steep, then a large change in relaxation time would result in a relatively small change in diffusivity. In other words, the counterions would display large variance in relaxation times even though their diffusivities are relatively close in magnitude. Other variables may then play a bigger role in influencing diffusivity, including the chemical structure of the ions (geometry, electronegativity, molecular volume, polarizability, etc.) and the glass transition temperature. On the other hand, if the curve is more shallow, then a small percentage change in relaxation time can result in a large percentage change in diffusivity. The ion association could play a significant role in diffusivity,

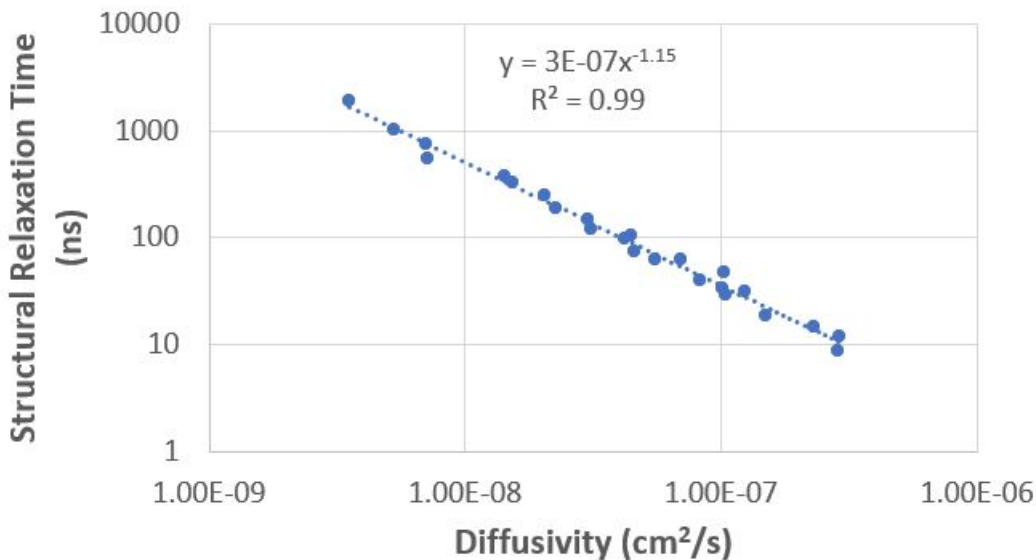


**Figure 6:** Structural relaxation time and diffusivity are negatively correlated. The steepness of this curve can provide useful insights into the factors that affect diffusivity.

but there could be other contributing factors as well. The power, in this case -1.15, can provide useful insights into the factors that affect diffusivity, and this relationship can be explored in future works.

## 4 Conclusions

In this work, diffusivity, ion-association lifetime, and structural relaxation time were computed for 8 different counterions in poly(1-butyl-3-vinylimidazolium). Diffusivities were on the order of  $10^{-7}$  cm<sup>2</sup>/s, and structural relaxation times and ion pair associations had similar rankings. In general, molecules with higher diffusivities tended to have lower ion pair associations: AlCl<sub>4</sub><sup>-</sup> and TFSI<sup>-</sup> had generally higher diffusivities and lower relaxation times. Structural relaxation time and diffusivity display an inverse correlation, with an R<sup>2</sup> value of 0.99. The next steps of this work are to compute the conductivity of these materials, examine the (inverse) relationship between conductivity and structural relaxation time, and normalize temperatures on the  $x$  axis by the glass transition temperature (inverse glass-

transition-normalized temperature or  $T_g/T$ ) to examine the extent of decoupling between ion mobility and segmental dynamics.

## References

1. *Polymerized Ionic Liquids*. [https://web.tuat.ac.jp/~ohno/research/research\\_e.html](https://web.tuat.ac.jp/~ohno/research/research_e.html).
2. Qian, W., Texter, J. & Yan, F. Frontiers in poly (ionic liquid) s: syntheses and applications. *Chemical Society Reviews* **46**, 1124–1159 (2017).
3. Mecerreyes, D. Polymeric ionic liquids: Broadening the properties and applications of polyelectrolytes. *Progress in Polymer Science* **36**, 1629–1648 (2011).
4. Keith, J. R., Mogurampelly, S., Aldukhi, F., Wheatle, B. K. & Ganesan, V. Influence of molecular weight on ion-transport properties of polymeric ionic liquids. *Physical Chemistry Chemical Physics* **19**, 29134–29145 (2017).
5. Mogurampelly, S., Keith, J. R. & Ganesan, V. Mechanisms underlying ion transport in polymerized ionic liquids. *Journal of the American Chemical Society* **139**, 9511–9514 (2017).
6. Iacob, C. *et al.* Polymerized ionic liquids: Correlation of ionic conductivity with nanoscale morphology and counterion volume. *ACS Macro Letters* **6**, 941–946 (2017).
7. Fan, F. *et al.* Ion conduction in polymerized ionic liquids with different pendant groups. *Macromolecules* **48**, 4461–4470 (2015).
8. Ogihara, W., Washiro, S., Nakajima, H. & Ohno, H. Effect of cation structure on the electrochemical and thermal properties of ion conductive polymers obtained from polymerizable ionic liquids. *Electrochimica Acta* **51**, 2614–2619 (2006).
9. Lee, M., Choi, U. H., Colby, R. H. & Gibson, H. W. Ion conduction in imidazolium acrylate ionic liquids and their polymers. *Chemistry of Materials* **22**, 5814–5822 (2010).
10. Choi, U. H. *et al.* Ionic conduction and dielectric response of poly (imidazolium acrylate) ionomers. *Macromolecules* **45**, 3974–3985 (2012).
11. La Cruz, D. S.-d. *et al.* Correlating backbone-to-backbone distance to ionic conductivity in amorphous polymerized ionic liquids. *Journal of Polymer Science Part B: Polymer Physics* **50**, 338–346 (2012).



12. Choi, U. H. *et al.* Dielectric and viscoelastic responses of imidazolium-based ionomers with different counterions and side chain lengths. *Macromolecules* **47**, 777–790 (2014).
13. Delhorbe, V. *et al.* Unveiling the ion conduction mechanism in imidazolium-based poly(ionic liquids): A comprehensive investigation of the structure-to-transport interplay. *Macromolecules* **50**, 4309–4321 (2017).
14. Choi, U. H. *et al.* Molecular volume effects on the dynamics of polymerized ionic liquids and their monomers. *Electrochimica Acta* **175**, 55–61 (2015).
15. Lappan, U. & Scheler, U. Influence of the Nature of the Ion Pairs on the Segmental Dynamics in Polyelectrolyte Complex Coacervate Phases. *Macromolecules* **50**, 8631–8636 (2017).
16. Allen, M. P. *et al.* Introduction to molecular dynamics simulation. *Computational soft matter: from synthetic polymers to proteins* **23**, 1–28 (2004).
17. Jorgensen, W. L., Maxwell, D. S. & Tirado-Rives, J. Development and testing of the OPLS all-atom force field on conformational energetics and properties of organic liquids. *Journal of the American Chemical Society* **118**, 11225–11236 (1996).
18. Sambasivarao, S. V. & Acevedo, O. Development of OPLS-AA force field parameters for 68 unique ionic liquids. *Journal of chemical theory and computation* **5**, 1038–1050 (2009).
19. Bhargava, B. & Balasubramanian, S. Refined potential model for atomistic simulations of ionic liquid [bmim][PF 6]. *The Journal of chemical physics* **127**, 114510 (2007).
20. Tsuzuki, S. *et al.* Molecular dynamics simulations of ionic liquids: cation and anion dependence of self-diffusion coefficients of ions. *The Journal of Physical Chemistry B* **113**, 10641–10649 (2009).
21. De Andrade, J., Böes, E. S. & Stassen, H. Computational study of room temperature molten salts composed by 1-alkyl-3-methylimidazolium cations force-field proposal and validation. *The journal of physical chemistry B* **106**, 13344–13351 (2002).

22. Canongia Lopes, J. N., Deschamps, J. & Pádua, A. A. Modeling ionic liquids using a systematic all-atom force field. *The Journal of Physical Chemistry B* **108**, 2038–2047 (2004).
23. Canongia Lopes, J. N. & Pádua, A. A. Molecular force field for ionic liquids composed of triflate or bistriflylimide anions. *The Journal of Physical Chemistry B* **108**, 16893–16898 (2004).